UNITED STATES DEPARTMENT OF THE INTERIOR

GEOLOGICAL SURVEY

Rb/Sr Isotopic Ratios in Selected Lower Crust-Upper Mantle Nodules from Colorado-Wyoming Kimberlites

By

Craig B. Smith,* M. E. McCallum, and C. E. Hedge

Open-File Report 82-178
1982

This report is preliminary and has not been reviewed for conformity with U.S. Geological Survey editorial standards.

*Presently affiliated with BPI Geophysics Unit, The University of Witwatersrand, Johannesburg 2001, South Africa

INTRODUCTION

Nineteen lower crustal and upper mantle nodules from kimberlites in Colorado and Wyoming were analyzed for whole-rock Rb-Sr concentrations and $^{87}Sr/^{86}Sr$ isotopic ratios. The samples, which represent eight different nodule types, were collected from seven different kimberlite pipes in the State Line district of the Colorado-Wyoming Front Range and the Iron Mountain district of the Wyoming Laramie Range (fig. 1). The nodule assemblage comprises eight granulites and one pyroxenite of lower crustal origin; and three eclogites, two peridotites, and five monomineralic megacrysts (>1 cm in diameter) of clinopyroxene and garnet of upper mantle origin. Brief descriptions of the samples are given in table 1, and major element chemistry of some samples is given in table 2 and shown on figure 2. Descriptions of host kimberlites are available in McCallum and Mabarak (1976), McCallum and others (1977), McCallum and Smith (1978), Smith (1977), and Smith and others (1979). The initial objectives of this study were to characterize the isotopic compositions of lower crustal nodules (hence the greater number of granulites), and to examine as many other types of material as possible to establish the amount of isotopic variability between rock types.

Rb-Sr analyses were performed by C. B. Smith by isotope dilution in the U.S. Geological Survey Isotope Geology Laboratory, Denver, Colo., under the supervision of C. H. Hedge. The samples were prepared by Kiyoto Futa for mass-spectrometry analysis. Analytical procedures are described in Peterman and others (1967, 1968). Electron microprobe mineral analyses were performed on selected nodules at the Carnegie

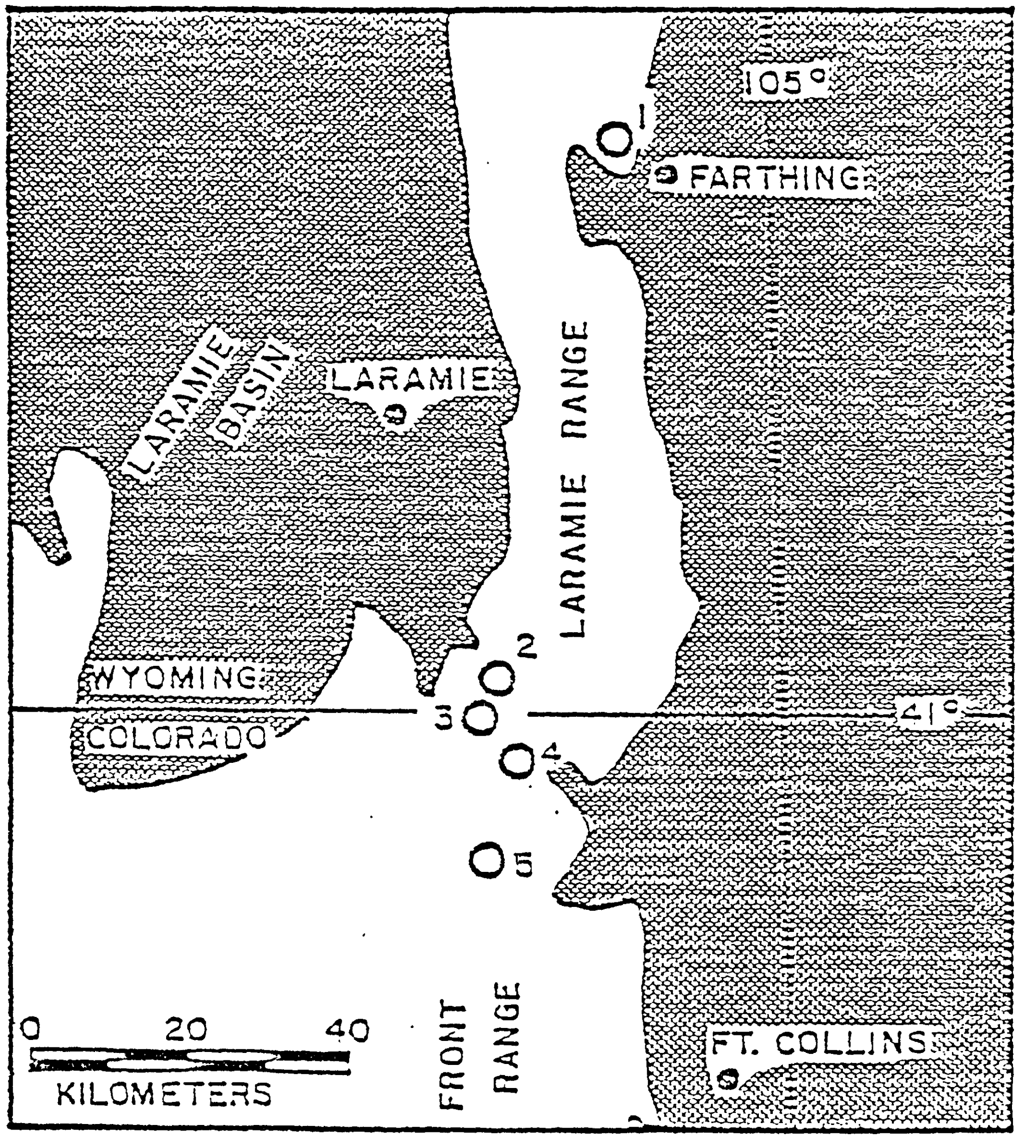

Figure 1. Location map of Colorado-Wyoming Front Range and Laramie Range kimberlites. 1-- Iron Mountain district; 2--Ferris and Aultman pipes; 3--Schaffer pipes; 4--Nix and Moen pipes; 5--Sloan pipes; 2,3,4 and 5 are collectively designated the State Line district.

Table 1. Descriptions of nodules analyzed for Rb and Sr. (IM, Iron Mountain; NX, Nix pipes; SD, Sloan pipes; SH, Schaffer pipes.)

Lower Crustal Rocks

SD2-LC1-- hypersthene granulite; medium-grained granular, plagioclase (An_{28-32}) and hypersthene with minor K-feldspar and ilmenite. Clotted texture defined by pyroxene.

SD2-LC18--- augite granulite; fine-grained granular plagioclase (An_{38}), augite and ilmenite with minor apatite. Feldspar locally sericitized or slightly kaolinitized (?). Moderately altered.

SD2-LC36-- hypersthene - augite granulite; fine-grained granular, plagioclase (An_{53-58}), augite, and hypersthene with minor K-feldspar, ilmenite and apatite. Minimal grain boundary alteration and minor alteration veinlets at margins.

SD2-LC37-- hypersthene-augite granulite; fine-grained granular, plagioclase (An_{45}), hypersthene and augite with minor ilmenite and apatite. Altered margins and thin alteration veinlets.

NX4-LC2-- hypersthene-augite granulite; fine-grained granular, plagioclase (An_{34}), hornblende, augite and hypersthene with minor K-feldspar and ilmenite.

SD2-LC28-- garnet granulite; granular to cataclastic, plagioclase (An_{38}), augite, and garnet with minor hypersthene, K-feldspar and apatite. Reasonably fresh.

SD2-E8-- garnet granulite; fine-grained granular, plagioclase (An_{30}), garnet and augite with minor ilmenite and rutile. Somewhat altered.

IM20-W5-- spinel clinopyroxenite; green interstitial hercynite in polygonal granoblastic clinopyroxene. Very fresh.

Eclogite (mantle-derived)

SH13-E4-- kyanite eclogite; medium-grained foliated granoblastic, clinopyroxene, garnet and kyanite. Intensely altered.

SD2-LC3-- kyanite-sanidine eclogite; medium-grained foliated granoblastic, clinopyroxene, garnet, kyanite and sanidine. Intensely altered.

SH13-E5-- eclogite; coarse-grained granoblastic, garnet and clinopyroxene. minor grain boundary alteration.

IM26-P2-- eclogite; medium-grained granoblastic, clinopyroxene garnet with accessory rutile. Moderate to intense grain boundary alteration.

Table 1. Continued

Peridotite (mantle-derived)

SD2-L1--medium-grained granular spinel lherzolite

SD2-L10--fine- to coarse-grained mosaic porphyroclastic garnet-spinel lherzolite of garnet websterite group affinity (McCallum and others, 1979)

Peridotites are relatively fresh but, minor grain boundary alteration is present.

Megacrysts (mantle-derived)

SD2-C3--Cr-rich clinopyroxene

IM7-C1-- Cr-poor clinopyroxene

SD2-G17--Cr-rich garnet

IM42-G7--Cr-poor garnet

IM7-G1--Cr-poor garnet

Megacrysts are relatively fresh although garnets may be altered along shear planes.

Table 2. Electron microprobe major oxide analyses for constituent minerals of selected nodules. (Analyses done by D. H. Eggler and C. B. Smith on a MAC 400 microprobe at the Carnegie Institution Geophysical Laboratory in Washington D. C.)

	SD2-LC18 (Pyroxene granulite)			SD2-LC3 (Garnet-kyanite granulite)			SD2-LC28 (Garnet granulite)		
	Clino-pyroxene	K-feldspar	Plagio-clase	Kyanite	Garnet	K-feldspar	Garnet	Clino-pyroxene	Plagio-clase
SiO_2	50.8	64.5	58.2	37.8	38.9	62.9	39.7	52.2	60.3
TiO_2	0.23	0.23	0.00	0.0	0.27	n.a.	0.04	0.44	n.a.
Al_2O_3	1.9	17.9	25.8	61.4	21.1	18.3	21.6	4.7	24.6
Cr_2O_3	0.00	0.00	n.a.	0.01	0.00	n.a.	0.07	0.02	n.a.
FeO	11.7	0.15	0.09	0.26	12.1	0.02	24.3	7.9	0.02
MnO	1.8	0.05	0.06	0.00	0.20	0.00	0.54	0.04	0.00
NiO	0.00	0.00	n.a.	0.02	0.00	n.a.	0.00	0.00	n.a.
MgO	12.0	0.00	0.02	0.03	1.2	0.01	9.1	12.6	0.02
CaO	20.0	0.38	8.1	0.00	25.7	0.00	5.9	19.9	6.8
Na_2O	0.4	0.98	6.2	0.00	0.13	0.69	0.01	2.0	6.8
K_2O	0.00	15.0	0.41	0.00	0.00	15.1	0.00	0.00	6.34
Total:	98.83	98.96	98.88	99.52	99.60	97.02	101.26	99.80	98.88

	IM20-W5 (Spinel clinopyroxenite)		SH13-E4 (Eclogite)		SH13-E5 (Eclogite)		IM26-P2 (Eclogite)		
	Clino-pyroxene	Spinel	Garnet	Clino-pyroxene	Garnet	Clino-pyroxene	Garnet	Clino-pyroxene	Rutile
SiO_2	49.6	0.20	42.0	54.8	42.5	55.4	40.3	55.8	0.11
TiO_2	0.81	0.02	0.00	0.00	0.00	0.00	0.01	0.18	84.1
Al_2O_3	7.4	64.1	22.9	11.1	23.1	12.9	22.1	8.9	1.2
Cr_2O_3	0.00	0.07	0.02	0.09	0.02	0.01	0.04	0.06	0.04
FeO	4.4	17.9	9.2	1.4	8.3	1.1	20.3	4.6	11.1
MnO	0.11	0.11	0.14	0.02	0.13	0.00	0.48	0.05	0.01
NiO	0.01	n.a.	0.02	0.13	0.03	0.07	0.00	0.00	0.01
MgO	14.2	17.0	15.0	11.4	17.8	10.2	11.9	10.3	0.49
CaO	23.1	0.16	11.8	16.5	9.3	14.7	5.6	14.8	0.01
Na_2O	0.32	0.00	0.08	4.6	0.02	5.3	0.00	5.4	0.00
K_2O	0.00	n.a.	0.00	0.00	0.00	0.00	n.a.	0.00	0.00
TOTAL:	99.95	99.95	101.15	100.04	101.2	99.68	100.73	100.09	97.07

Table 2 - Cont.

	SD2-L1 (Spinel lherzolite)				SD2-L10 (Garnet-spinel lherzolite)			
	Spinel	Clino-pyroxene	Olivine	Ortho-pyroxene	Garnet	Clino-pyroxene	Olivine	Ortho-pyroxene
SiO_2	0.08	54.4	42.3	57.1	42.6	54.0	41.8	57.7
TiO_2	0.00	0.00	0.00	0.00	0.10	0.51	0.00	0.11
Al_2O_3	42.0	2.6	0.00	2.9	22.5	4.4	0.02	1.4
Cr_2O_3	27.5	0.8	0.00	0.52	1.6	1.2	0.09	0.32
FeO	11.6	1.2	7.0	4.6	10.5	2.3	8.0	6.1
MnO	0.19	0.09	0.10	0.13	0.6	0.09	0.14	0.13
NiO	0.13	0.04	0.38	0.07	0.00	0.03	0.36	0.04
MgO	18.9	17.1	52.5	35.9	19.5	15.3	51.9	35.5
CaO	0.00	23.3	0.01	0.17	4.9	20.7	0.04	0.30
Na_2O	0.02	0.84	0.00	0.01	0.01	2.1	0.02	0.00
K_2O	n.a.	n.a.	n.a.	n.a.	n.a.	n.a.	n.a.	n.a.
Total:	100.42	100.37	100.29	101.40	102.31	100.63	102.37	101.60

MEGACRYSTS

	SD2-G17 Cr-rich Garnet	IM42-G7 Cr-poor Garnet	SD2-C3 Cr-rich CPX	IM7-C1 Cr-poor CPX
SiO_2	39.7	42.3	55.2	54.7
TiO_2	0.68	0.61	0.12	0.25
Al_2O_3	13.1	21.5	1.1	2.3
Cr_2O_3	12.3	1.1	1.5	0.3
FeO	6.8	9.7	2.8	4.6
MnO	0.39	0.34	0.14	0.08
NiO	0.00	0.00	0.05	0.10
MgO	18.4	20.5	19.2	19.5
CaO	8.2	4.2	19.3	16.1
Na_2O	0.06	0.09	1.0	1.4
K_2O	0.00	0.00	0.04	0.03
Total:	99.63	100.34	100.45	99.36

FeO = FeO + Fe_2O_3

n.a. = not analyzed

Figure 2. Compositions (in mole percent) of clinopyroxene (---), garnet (— — —) and orthopyroxene (— - —) in nodules analyzed for Rb and Sr, plotted on a Ca-Mg-Fe ternary diagram. Coexisting phases connected by tie lines.

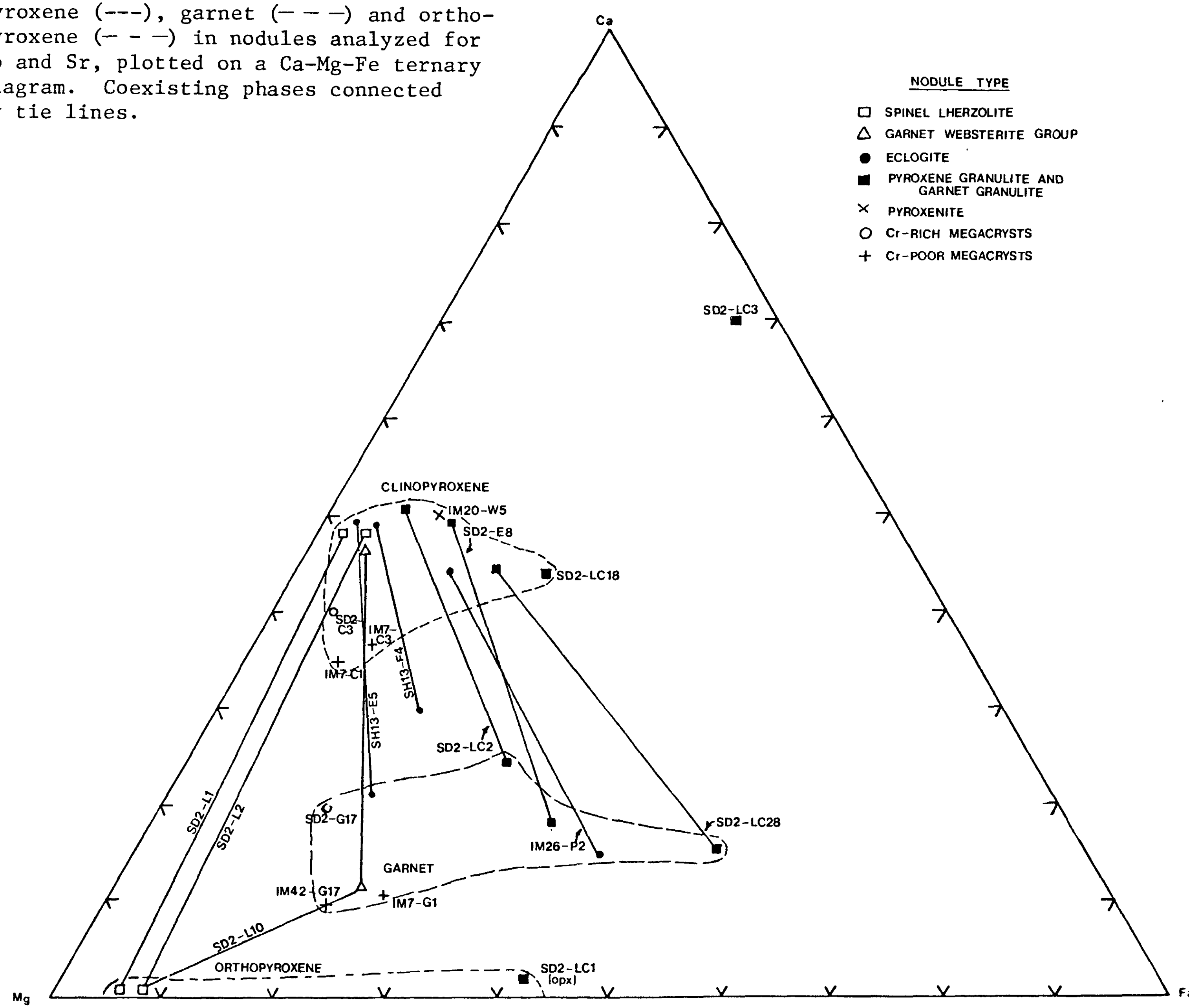

Institution Geophysical Laboratory in Washington, D.C., by D. H. Eggler and C. B. Smith.

Rb-Sr SYSTEMATICS AND DISCUSSION

Rb and Sr concentrations obtained from whole rock sample analysis are lowest in the pyroxenite, peridotites, and clinopyroxene and garnet megacrysts (Rb = 0.15 to 10.3 ppm; Sr = 11 to 126 ppm) (table 3, fig. 3). One eclogite nodule (sample SH13-E5) also contains low Rb and Sr values (Rb = 1.78 ppm, Sr = 80.32 ppm), but the other eclogites are characterized by higher Sr values (324 and 452 ppm) accompanying the low Rb values (4.31 and 4.51 ppm). The granulites consistently contain higher and more variable Rb and Sr than other nodules (Rb = 21.8 to 153 ppm, Sr = 547 to 4465 ppm) (table 3, fig. 3).

$^{87}Sr/^{86}Sr$ and $^{87}Rb/^{86}Sr$ ratios are given in table 3 and are shown on a Sr evolution diagram in figure 4. The scatter of data is large; $^{87}Sr/^{86}Sr$ ranges from .70348 to .71658, and $^{87}Rb/^{86}Sr$ ranges from .003 to .705. High $^{87}Sr/^{86}Sr$ and (or) high $^{87}Rb/^{86}Sr$ does not in all cases correspond with high Sr and (or) Rb. The two clinopyroxene megacrysts (one Cr-poor and one Cr-rich) and one eclogite nodule (IM26-P2) have the lowest $^{87}Sr/^{86}Sr$ ratios (.70349 to .70360). The one websterite group peridotite (SD2-L10) has the highest and least precise $^{87}Sr/^{86}Sr$ ratio (.71658 and .71315 for two determinations). $^{87}Sr/^{86}Sr$ ratios of all other samples cluster between .7050 and .7109.

Isotopic ratios are, as a group, similar to ranges of clinopyroxene megacrysts and kimberlite from South Africa analyzed by Kramers (1977).

Table 3. Rb-Sr concentrations and isotopic ratios. (Most analyses are of whole rock material although some represent leached residual whole rock and accompanying leach fraction material).

	Rb(ppm)	Sr(ppm)	Rb/Sr	$^{87}Sr/^{86}Sr$	$^{87}Rb/^{86}Sr$	1/Sr
Pyroxene Granulites						
SD2-LC1	102.	4465	.023	.71020	---	.00022
SD2-LC1 (residual)	77.2	657.	.117	.70784	.340	.00152
SD2-LC1 (leach)	---	6391.	---	.70854	---	.00016
SD2-LC18	153.	3265	.047	.70828	.136	
SD2-LC36	43.0	722	.060	.70674	.172	
SD2-LC37	106.	547	.194	.70832	.562	
NX4-LC2	22.0	923	.024	.70716	.069	
Garnet Granulites						
SD2-LC3	25.2	2531	.010	.70850	---	.00040
SD2-LC3 (residual)	16.4	349	.047	.70543	.136	.00287
SD2-LC3 (residual)	---	365	---	.70560	---	.00274
SD2-LC3 (leach)	---	3952	---	.70832	---	.00025
SD2-LC28	2.18	570	.038	.70527	.111	
SD2-E8	36.8	1092	.034	.70674	.098	.00092
SD2-E8 (residual)	---	766	---	.70560	---	.00130
Pyroxenite						
IM20-W5	3.99	74.7	.053	.71009	.155	
Kyanite Eclogite						
SH13-E4	4.31	325	.013	.70849	.037	
Eclogite						
SH13-E5	1.78	80.3	.022	.70683	.064	
IM26-P2	4.51	452	.010	.70360	.029	
Peridotites						
SD2-L1 (spinel)	3.29	29.8	.111	.70956	.320	.03360
SD2-L1 (spinel) (residual)	2.60	16.8	.155	.70599	.448	.05949
SD2-L10 (garnet-spinel) (1st Run)	6.17	25.9	.243	.71658	.705	
(2nd Run)	6.17	25.5	.242	.71315	.702	
Megacrysts						
SD2-C3 (Cr-rich cpx)	1.83	110	.017	.70348	.048	
IM7-C1 (Cr-poor cpx)	0.15	126	.001	.70360	.003	
SD2-G17 (Cr-rich gar.)	10.3	42.2	.243	.70798	.704	
IM7-G1 (Cr-poor gar.) (residual)	1.55	≈11.0	~.141	---	---	
IM42-G7 (Cr-poor gar.)	2.12-3.60	21.9	.097-.164	.70744	.281-.476	

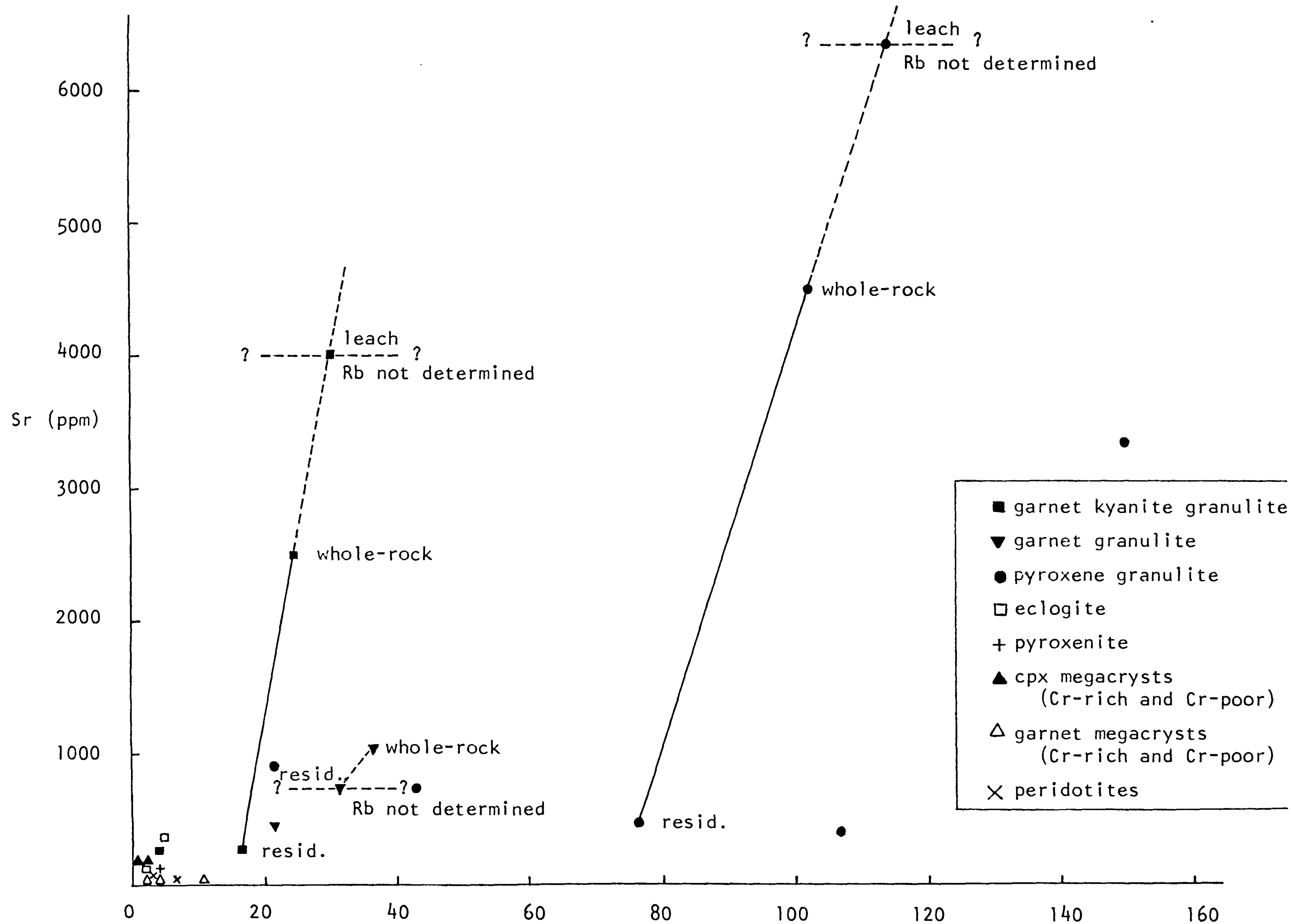

Figure 3. Sr-Rb plots (in parts per million). Tie lines connect whole-rock, whole-rock after leaching (residual), and(or) leach fraction.

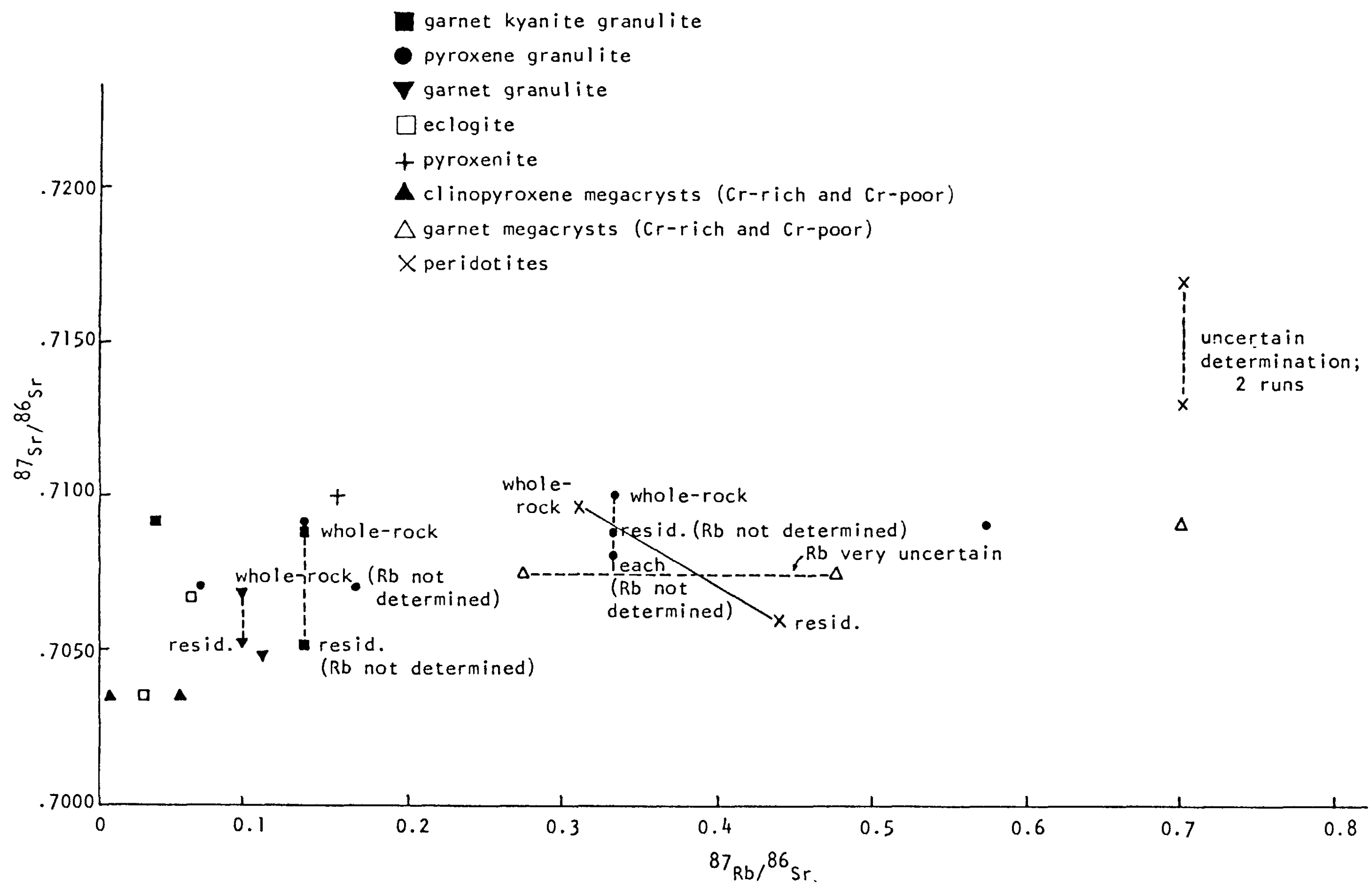

Figure 4. Sr evolution diagram ($^{87}Sr/^{86}Sr$ versus $^{87}Rb/^{86}Sr$). Tie lines connect whole-rock, whole rock after leaching (residual), and(or) leach fraction.

$^{87}Rb/^{86}Sr$ ratios are somewhat lower than those of South African kimberlite autoliths determined by Barrett (1975), although $^{87}Sr/^{86}Sr$ ratios are similar.

The analyses show that mantle-derived materials (peridotite, eclogite, and megacrysts) have generally lower Rb and Sr abundances than lower crustal nodules (pyroxene granulite and garnet granulite), with the exception of the pyroxenite (IM20-W5) which is of probable lower crustal origin (tables 1 and 3; fig. 3). Such a trend is to be expected in that crustal rocks are generally enriched in incompatible elements relative to mantle rocks. However, the isotopic ratios of the samples do not display any such regularity (fig. 4, table 3). The data scatter shown in figures 3 and 4 is caused by two factors: the variety of nodule types analyzed and the partially altered nature of most samples.

Analyses of leached residual whole-rock and some accompanying leach fractions, as well as whole rock material of selected samples (table 3), indicate that the isotopic compositions of the nodules probably reflect alteration processes. Thin sections of most nodules reveal grain boundary alteration films, and some samples contain veinlets of carbonate-sericite(?)-serpentine-clay mixtures (e.g., SD2-LC1, SD2-LC3). Only one polygranular nodule (IM20-W5) appears to be completely free of alteration, as also are the two clinopyroxene megacrysts. It is apparent that most nodules were not closed systems with respect to Rb and Sr, and isotopic contamination is thought to have resulted from invasion of fluids along grain boundaries and (or) fractures. The analyses reported herein are whole-rock fractions; thus grain boundary contaminants could not be entirely eliminated from the sample. Carefully prepared mineral separates could possibly yield more accurate isotopic data providing that diffusion exchange processes have not been severe. The clinopyroxene megacrysts were probably less affected by alteration in that they are single crystals and thus have no grain boundaries to serve as channelways for fluids. The low isotopic ratios of the two samples (table 3; figs. 4 and 5) probably represent reliable values. This contention is supported by the extremely low Rb/Sr and $^{87}Rb^{86}Sr$ ratios for the Cr-poor clinopyroxene megacryst. Such values are generally characteristic of more primitive mantle material, and these nodules have been interpreted as products of a fractionating magma, separated during partial melting of essentially undepleted mantle peridotite from the asthenosphere, that has upwelled in a diapir to a depth of approximately 150-200 km (Eggler and others, 1979). Such partial melts are believed to be associated with protokimberlite magmas.

Alteration in the garnet megacrysts is more difficult to assess because the garnets are commonly partially sheared. Chemical determinations for the garnets are less precise than for clinopyroxenes. Analyses on different parts of the same sample may give diverse results (see sample IM42-G7, table 3 and fig. 4). However, general relative trends appear to correlate reasonably well with those of clinopyroxene megacrysts considering that Cr-poor garnets contain much lower levels of Rb and have lower Rb/Sr and $^{87}Rb/^{86}Sr$ ratios than the Cr-rich garnet (table 3).

In figures 3, 4, 5, and 6, the whole-rock, residual whole-rock, and leach fractions of individual samples are connected by lines. Leaching of whole-rock with dilute HCl removes easily extractable material such as grain boundary carbonates, and ideally removes the isotopic component

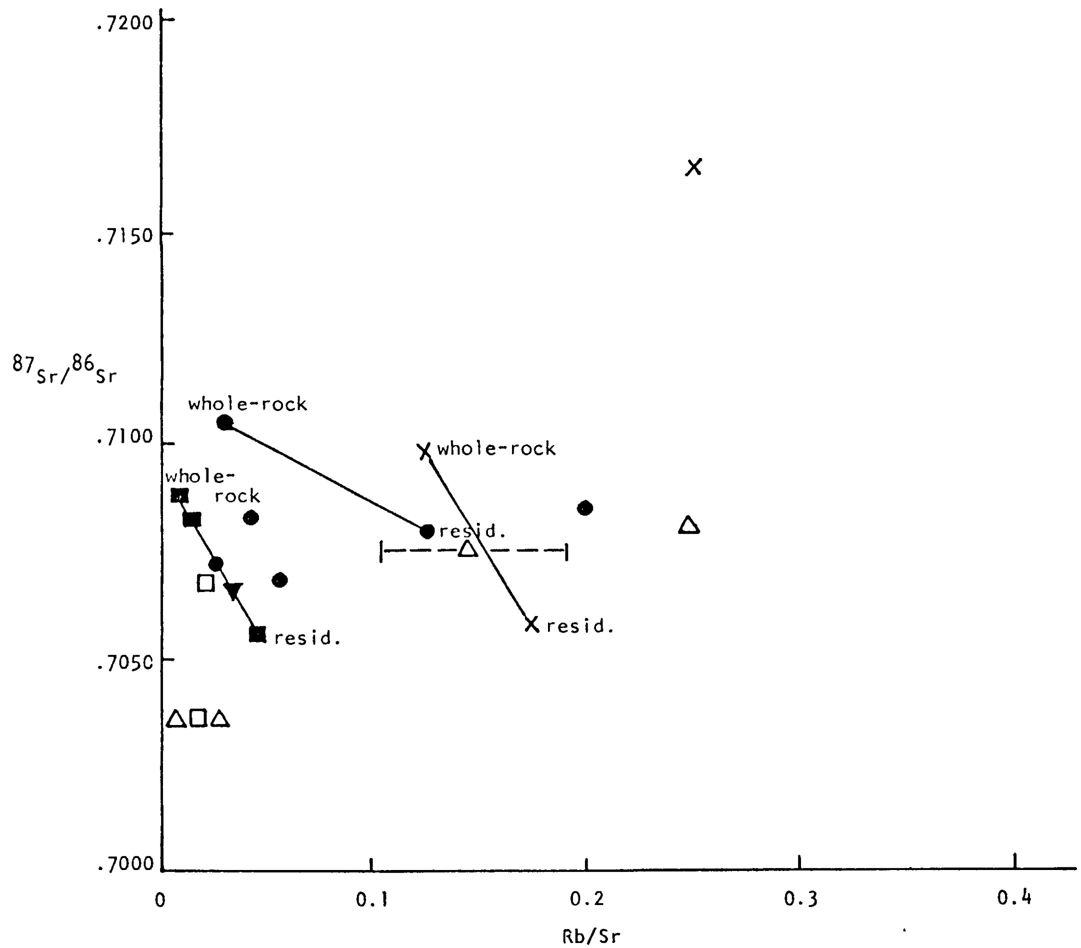

Figure 5. $^{87}Sr/^{86}Sr$ versus Rb/Sr plots. Tie lines connect whole-rock, whole rock after leaching (residual), and(or) leach fraction. Symbols same as Figure 4.

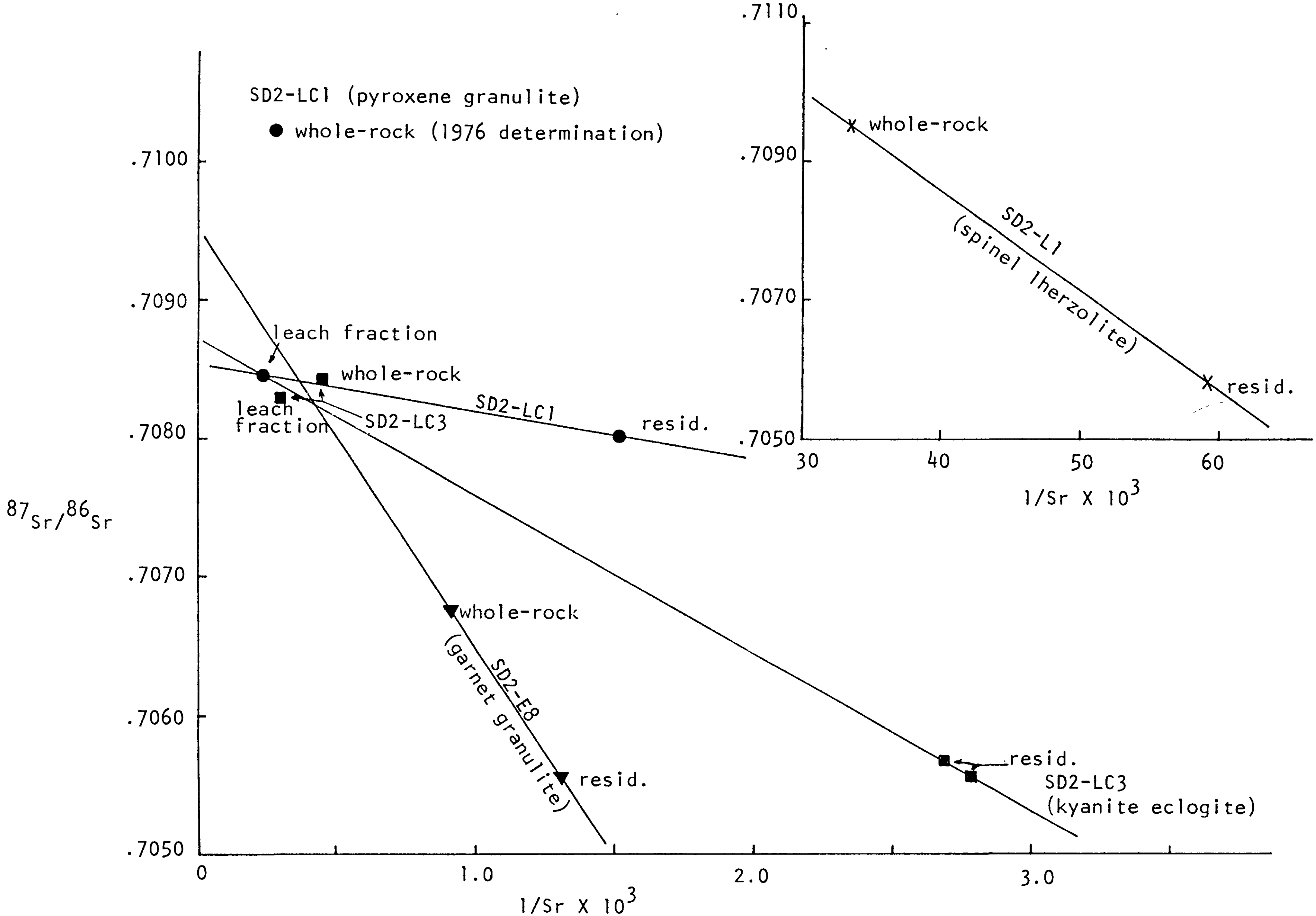

Figure 6. $^{87}Sr/^{86}Sr$ versus 1/Sr (Sr as parts per million). Tie lines connect whole-rock, whole-rock after leaching (residual), and(or) leach fraction.

contributed by alteration. The term "resid" in figures 3, 4, 5, and 6 indicates the whole-rock isotopic composition of the sample after leaching; "leach" indicates the isotopic composition of the material that was extracted. Figures 3, 4, 5, and 6 clearly indicate that the isotopic compositions are altered. Tie lines for isotopic data plots of similar slope and magnitude between whole rock and leached residual whole rock fractions (figs. 5 and 6), as well as the similarity of alteration of mantle derived and lower crustal rocks, suggest that alteration of all samples occurred in a single event. Figure 6 suggests that the alteration medium had a high $^{87}Sr/^{86}Sr$ isotopic composition of .708 to .709. This range would be lowered slightly by adjustment of isotopic ratios to the emplacement age of kimberlite (about 400 m.y. - Naeser and McCallum, 1977; Smith, 1979), but ratios would not fall below about .707.

The carbonatized nature of many Front Range kimberlites and included nodules indicates that rising, volatile-rich, kimberlite magma contained carbonatitic components. $^{87}Sr/^{86}Sr$ ratios of the analyzed nodules, especially the granulites, are similar to ratios in carbonatites from Africa, North America, and Europe which range from .7034 to .7088 (Hamilton, 1965). The majority of alteration that has affected xenoliths in the Colorado-Wyoming kimberlites probably occurred within the intruding kimberlite magma. This alteration could have occurred at or near the base of the crust, and, in that situation, it is likely that this event was responsible for complete carbonatization of some nodules as suggested by Nixon and Boyd (1973) and McCallum (1976). Strontium isotopic compositions of kimberlite or carbonate-rich kimberlite from the Colorado-Wyoming Front Range have not yet been determined, but the $^{87}Sr/^{86}Sr$ ratios should be similar to most of the analyzed nodules and carbonatites.

Although all of the rocks represented in this study are not genetically related, petrography and mineral chemistry show some relationships and clearly show internal similarities within distinct sample groups. For example, the pyroxene granulites and garnet granulites do appear to be genetically related. Relationships between some of the other sample groups, however, are less definitive (e.g., eclogite versus peridotite). Because of the uncertain relationships between many samples and the nature and intensity of nodule alteration, as well as the qualitative aspects of the analytical leaching techniques, isotopic ratios cannot be determined accurately. Viable isochrons cannot be constructed, and initial $^{87}Sr/^{86}Sr$ ratios and ages cannot be determined. Recalculation of $^{87}Sr/^{86}Sr$ ratios to the age of kimberlite emplacement (approximately 400 m.y.) lowers the ratios slightly, but does not markedly reduce the scatter of the data (table 4). However, if an initial $^{87}Sr/^{86}Sr$ ratio of .702 (a reasonable value for basalts and mantle-derived nodules) is used, relative ages can be calculated for individual samples. Geologically reasonable ages, obtained by such calculations, range from 600 to 3,700 m.y. There is no chemical or petrographic evidence that any of these nodules are related to or were affected by Tertiary magmatic events of the type that were active in the Colorado Mineral Belt or in the nearby northern Colorado lineament area (McCallum and Naeser, 1977).

Table 4. $^{87}Sr/^{86}Sr$ ratios calculated to age of kimberlite emplacement (~400 m.y.).

Sample	$^{87}Sr/^{86}Sr$ (now)	$^{87}Sr/^{86}Sr$ (emplacement)
SD2-LC1 (resid.)	.70784	.70595
SD2-LC18	.70828	.70752
SD2-LC36	.70674	.70578
SD2-LC37	.70832	.70520
NX4-LC2	.70716	.70677
SD2-LC3 (resid.)	.70543	.70467
SD2-LC28	.70527	.70465
SD2-E8	.70674	.70620
IM20-W5	.71009	.70923
SH13-E5	.70683	.70647
IM26-P2	.70360	.70344
SD2-L1 (resid.)	.70599	.70350
SD2-L10	.71315	.71266
SD2-C3	.70348	.70321
IM7-C1	.70360	.70358

Calculations performed using following formula:

$$^{87}Sr/^{86}Sr - {}^{87}Rb/^{86}Sr\ (\lambda)\tau \approx {}^{87}Sr/^{86}Sr_{\text{(emplacement)}}$$

$$\lambda = 1.39 \times 10^{-11}/yr$$

$$\tau = 4.0 \times 10^{8}$$

ACKNOWLEDGMENTS

We wish to extend our appreciation to Kiyoto Futa of the U.S. Geological Survey for his help in preparing samples for mass spectrometry analyses. We are also grateful to D. H. Eggler for his help in obtaining electron microprobe analyses of selected nodular material, and to the Carnegie Institution Geophysical Laboratories in Washington, D.C., for the use of their microprobe facilities. The study was supported in part by the Earth Sciences Section of the National Science Foundation (Contracts EAR 74-13098 A01 and EAR 7810775).

REFERENCES

Barrett, D. R., 1975, The genesis of kimberlite and associated rocks--Strontium isotopic evidence: Proceedings of the First International Kimberlite Conference, Physics and Chemistry of the Earth, v. 9, p. 637-653.

Eggler, D. H., McCallum, M. E., and Smith, C. B., 1979, Megacryst assemblages in kimberlite from northern Colorado and southern Wyoming--Petrology, geothermometry-barometry, and areal distribution: Proceedings of the Second International Kimberlite Conference, American Geophysical Union, v. 2, p. 213-226.

Hamilton, E. I., 1965, Applied Geochemistry: London, Academic Press, 267 p.

Kramers, J. D., 1977, Lead and strontium isotopes in Cretaceous kimberlites and mantle-derived xenoliths from southern Africa: Earth and Planetary Science Letters, v. 34, p. 419-431.

McCallum, M. E., 1976, An emplacement model to explain contrasting mineral assemblages in adjacent kimberlite pipes: Journal of Geology, v. 84, p. 673-684.

McCallum, M. E., Eggler, D. H., Coopersmith, H. G., Smith, C. B., and Mabarak, C. D., 1977, Field Guide, Colorado-Wyoming State Line Kimberlite District: Second International Kimberlite Conference, Santa Fe, New Mexico, 23 p.

McCallum, M. E., Kirkley, M. B., Padgett, J. L., and Eggler, D. H., 1979, Textural and mineral compositional ranges of ultramafic nodules from kimberlites of northern Colorado and southern Wyoming: Kimberlite Symposium II, Cambridge, England, p. 1-5.

McCallum, M. E., and Mabarak, C. D., 1976, Diamond in State-Line kimberlite diatremes, Albany County, Wyoming, and Larimer County, Colorado: Geological Survey of Wyoming Report of Investigations no. 12, 36 p.

McCallum, M. E., and Naeser, C. W., 1977, Fission track ages of Tertiary intrusive rocks in the Manhattan mining district, northern Front Range, Colorado: Isochron West, no. 18, p. 1-4.

McCallum, M. E., and Smith, C. B., 1978, Minor and trace element contents of kimberlite of the Front Range, Colorado and Wyoming: U.S. Geological Survey Open-File Report 78-1011, 23 p.

Naeser, C. W., and McCallum, M. E., 1977, Fission-track dating of kimberlite zircons [abs.]: Extended Abstracts, Second International Kimberlite Conference, Santa Fe, New Mexico.

Nixon, P. H., and Boyd, F. R., 1973, Carbonated ultrabasic nodules from Sekameng, in Nixon, P. H., ed., Lesotho Kimberlites: Lesotho National Development Corporation, Maseru, Lesotho, p. 190-196.

Peterman, Z. E., Doe, B. R., and Bartel, A. J., 1967, Data on the rock GSP-1 (granodiorite) and the isotope-dilution method of analyses for Rb and Sr: U.S. Geological Survey Professional Paper 575-B, p. 181-186.

Peterman, Z. E., Hedge, C. E., and Braddock, W. A., 1968, Age of Precambrian events in the northeastern Front Range, Colorado: Journal of Geophysical Research, v. 73, p. 2277-2296.

Smith, C. B., 1977, Kimberlite and mantle derived xenoliths at Iron Mountain, Wyoming: Fort Collins, Colorado State University, unpublished M.S. thesis, 218 p.

______1979, Rb-Sr mica ages of various kimberlite: Kimberlite Symposium II, Cambridge, England, p. 61-64.

Smith, C. B., McCallum, M. E., Coopersmith, H. G., and Eggler, D. H., 1979, Petrochemistry and structure of kimberlites in the Front Range and Laramie Range, Colorado-Wyoming: Proceedings of the Second International Kimberlite Conference, American Geophysical Union, v. 1, p. 178-189.